Analytica Chimica Acta xxx (2018) 1–9

Contents lists available at ScienceDirect

Analytica Chimica Acta

journal homepage: www.elsevier.com/locate/aca

A highly sensitive peptide-based biosensor using $NiCo_2O_4$ nanosheets and g-C_3N_4 nanocomposite to construct amplified strategy for trypsin detection

Yanyu Lin [a, 1], Rongkai Shen [b, 1], Nannan Liu [a], Huan Yi [c], Hong Dai [a, *], Jianhua Lin [b, **]

[a] College of Chemistry and Materials, Fujian Provincial Key Laboratory of Advanced Materials Oriented Chemical Engineering, Fujian Normal University, Fuzhou, Fujian, 350108, China
[b] The First Affiliated Hospital of Fujian Medical University, Fuzhou, Fujian, 350002, China
[c] Fujian Provincial Maternity and Children's Hospital, Affiliated Hospital of Fujian Medical University, Fuzhou, Fujian, 350108, China

HIGHLIGHTS

- A peptide-based biosensor was constructed based on superstructure to detect trypsin.
- This is the first time $NiCo_2O_4$ superstructure was used in designing a peptide-based biosensor.
- The proposed peptide-based biosensor shows extraordinary performance in low detection limit and wide linear range.

GRAPHICAL ABSTRACT

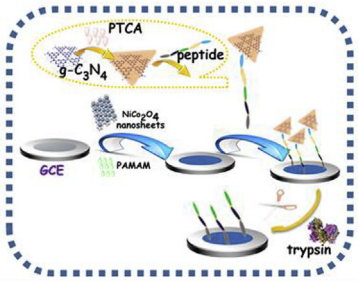

ARTICLE INFO

Article history:
Received 21 March 2018
Received in revised form
11 June 2018
Accepted 13 June 2018
Available online xxx

Keywords:
$NiCo_2O_4$ nanosheets
Peptide-based sensor
Trypsin
g-C_3N_4 nanocomposite

ABSTRACT

Here, a simple electrochemical biosensor was proposed based on the specific recognition between trypsin and peptide. Initially, $NiCo_2O_4$-PAMAM nanocomposite was casted on the bare electrode to achieve the electrochemical signal amplification in 0.1 mM $[Ru(NH_3)_6]^{3+}$ solution owing to the great electronic conductivity and high electrochemical activity induced by the special structure of $NiCo_2O_4$ nanosheets (Ni^{3+} cations in octachedral sites of the Co_3O_4). Subsequently, a declined electrochemical signal was obtained when g-C_3N_4 labeled peptide composites were anchored on the electrode. However, after trypsin was added into solution and incubated with the biosensor, the electrochemical signal was re-promoted. Therefore, the as-synthesized biosensor could realize the sensitive detection of trypsin by virtue of the specific recognition between trypsin and peptide. As a result, the developed peptide-based exhibited a linear range from 10^{-10} to 10^{-4} mg mL^{-1} with an ultralow detection limit of 10^{-10} mg mL^{-1}, providing sensitive analytical performance and acceptable application potential in clinical test and disease diagnosis due to its high stability, excellent selectivity, acceptable reproducibility and accurate signal output.

1. Introduction

Trypsin, a kind of serine protease produced by the pancreas, has been widely studied in recent years. Trypsin is of vital importance

* Corresponding author.
** Corresponding author.
E-mail addresses: dhong@fjnu.edu.cn (H. Dai), 120101515@qq.com (J. Lin).
[1] The author contributed to the work equally and should be regarded as co-first author.

https://doi.org/10.1016/j.aca.2018.06.040
0003-2670/

in controlling the function of pancreatic exocrine due to the active form of trypsin could lead to the transformation of other pancreatic proenzymes into active forms [1]. Therefore, as it was reported, trypsin has been widely used in biochemical applications, identifying protein in peptide sequencing techniques and diagnostic tests of pancreatic function, because it could specifically and effectively self-cleave proteins on the C-terminal side of arginine or lysine residues [1]. Besides, it is known that the level of trypsin also could serve as a reliable and specific biomarker for some diseases, such as cystic fibrosis, chronic pancreatic and even cancer [2]. Accordingly, it is significant to detect the trypsin activities in the fields of the physiological and pathological diagnosis [3]. Nowadays, a variety of methods have been developed to detect trypsin, such as radioimmunoassay [4], enzyme-linked immunosorbent assay (ELISA) [5], gelatin-based film technique [6] and colorimetric assay [7]. Nevertheless, these traditional methods require not only multifarious and time-consuming preparations of samples, but also specialized instruments and trained personnel. Thus designing a simple and quick biosensor for the sensitive determination of trypsin is especially important.

Several biosensors based on different methods, such as Quartz Crystal Microbalance (QCM) [8], fluorescent [9] and electrochemical [10] methods have been developed to detect trypsin. However, these methods still could not meet the requirement of low detection limit and satisfying linear range. For example, M. Stoytcheva et al. reported a sensitive trypsin activity evaluation applying a nanostructured QCM-sensors but its detection limit can be further improved [1]. In addition, although an optical sensitive nanoprobe (Mn: ZnSe d-dots-Arg_6) for trypsin determination and its inhibitor response was fabricated based on the fluorescence quenching by Xue Gao et al., its liner range was only from 0.1 to 12.0 $\mu g\ mL^{-1}$ [11]. Recent years, using short binding peptides as substrates has been considered as a promising way to detect enzyme because of their unique merits of stable, reliable, cost-effective, resistant to harsh environments and more amendable to engineering at the molecular level [12]. However, considering rare reports of peptide-based biosensor for trypsin detection have been developed till now, in this work, a peptide-based platform designed by electrochemical approach was fabricated to achieve sensitive detection for trypsin.

In the electrochemical peptide-based sensing system, selecting proper materials to realize the immobilization of peptides and the amplification of electrochemical signal is the first thing should be considered. In the last few years, nanomaterials have attracted considerable attention due to its charming properties of biocompatibility, nontoxicity, environmental-friendly, especially the excellent electrochemical catalytic activity, which was significant in designing signal amplification strategies. Among them, the particular properties of transition metal-based nanomaterials make them the potential candidates to be chosen. $NiCo_2O_4$, a kind of mixed transition metal oxide with spinel structure has drawn considerable attention in many fields due to its much better electronic conductivity and higher electrochemical activity than single nickel oxides or cobalt oxides [12,13]. Besides, other advantages of better electrochemical catalytic activity, biocompatibility, nontoxicity, and environmental-friendly [13] made the structure of $NiCo_2O_4$ be further investigated. Compared with other structures like $NiCo_2O_4$ nanoparticle, nanotubes and $NiCo_2O_4$ cluster, $NiCo_2O_4$ superstructure shows much better performance because its larger surface area could effectively contact the electrolyte and electrode materials and its better conductivity could accelerate transport rate of ions/electrons in the electrode and the interface of electrode/electrolyte [14]. Even so, the superstructure of $NiCo_2O_4$ has not been applied in designing electrochemical biosensor. Herein, $NiCo_2O_4$ superstructure was synthesized by a similar way with Hejun Li group [15] and employed as sensing matrix to amplify electrochemical signals. Additionally, to further promote the performance of $NiCo_2O_4$, PAMAM was introduced to realize the functionalization of $NiCo_2O_4$. The space structures of PAMAM dendrimers are highly branched three-dimensional macromolecules with massive functional amino-groups (-NH_2), which enable $NiCo_2O_4$-PAMAM nanocomposites film to capture more peptides. Considering the assemble ability between peptides and 3,4,9,10-perylene tetracarboxylic acid (PTCA) and the π-π conjugation between the PTCA and g-C_3N_4 [17], PTCA was employed to connect peptides and g-C_3N_4 which could quench the electrochemical signal [18].

In this work, a sensitive electrochemical peptide-based sensor was developed based on the amplified strategy of $NiCo_2O_4$ nanosheets. The fabricated process of the biosensor was presented in Scheme 1. First of all, $NiCo_2O_4$-PAMAM nanocomposite was modified on the bare glassy carbon electrode, which could effectively promote the electrochemical signal owing to the excellent conductivity of $NiCo_2O_4$. Moreover, the large surface area of $NiCo_2O_4$ [19] and the highly branched 3D structure of PAMAM [16] provided more active sites for the anchor of peptides to further expand the range of assay. Subsequently, the peptides were labeled with PTCA functionalized g-C_3N_4 via the π-π stacking between the PTCA and g-C_3N_4 and then linked to $NiCo_2O_4$-PAMAM nanocomposite, leading to a distinctly declined electrochemical response due to the quench effect of g-C_3N_4. Nevertheless, after the incubation between trypsin and peptides, a remarkably raised electrochemical signal was realized, providing an effective electrochemical strategy for the sensitive determination of trypsin. The reason could be explained by the specific recognization between the peptide and trypsin, which triggered the releasing of g-C_3N_4 from the electrode and thus resulted in the electrochemical signal recovered proportionally to the concentration of trypsin. In a word, the peptide-based biosensor was first proposed on the basis of $NiCo_2O_4$ superstructure as the electrochemical signal amplification matrix to realize the fast, sensitive, and accurate detection of trypsin activity in real samples, showing promising application in clinical test and disease diagnosis.

2. Experimental

2.1. Materials and reagents

Peptide (CAGRAAADAD) was purchased from Biodee

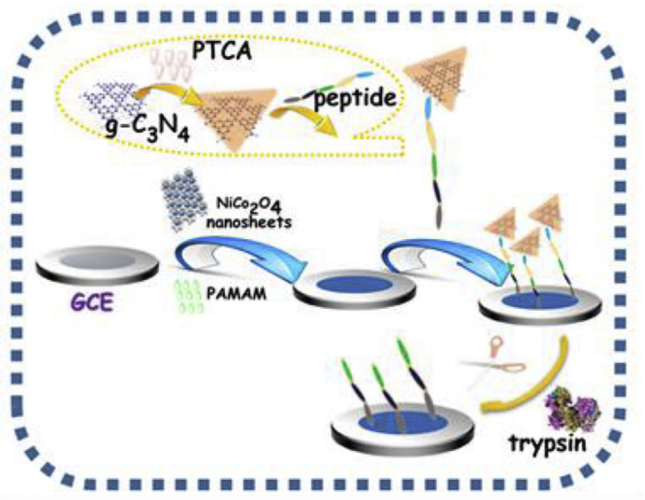

Scheme 1. Schematic illustration the process of fabrication of peptide-based biosensor for sensing trypsin.

Please cite this article in press as: Y. Lin, et al., A highly sensitive peptide-based biosensor using $NiCo_2O_4$ nanosheets and g-C_3N_4 nanocomposite to construct amplified strategy for trypsin detection, Analytica Chimica Acta (2018), https://doi.org/10.1016/j.aca.2018.06.040

Biotechnology Co. Ltd. (Beijing). Trypsin and lysozyme, alpha fetoprotein (AFP), and horseradish peroxidase (HRP) were bought from Beijing Bioss Biology Technology Ltd. (China), and bovine serum albumin (BSA) was purchased from Sino-American Biotechnology Co., Ltd. Poly(amidoamine) dendrimer (PAMAM), Hexaammineruthnium (III) chloride, and 3,4,9,10-perylene tetracarboxylic acid (PTCA) were bought from Aladdin Inc. (Shanghai, China).1-Ethyl-3-(3-dimethylaminopropyl)carbodiimide (EDC) was purchased from Sigma (St. Louis, MO, USA), g-C_3N_4 was synthesized according to previous report [18]. Human serum samples were supplied by the local hospital and human urine samples were collected from healthy volunteers. Phosphate buffer solution (PBS) was prepared by mixing 0.1 M NaH_2PO_4 and 0.1 M Na_2HPO_4 under monitoring of PHS-3C exact digital pH metre (Shanghai, China). Trihydroxymethyl aminomethane (Tris), HCl, NaOH and other reagents were of analytical grade and used without further purification.

2.2. Apparatus and measurements

Scanning electron microscopy (SEM, SU8000 instrument) and Transmission electron microscopy (TEM, FEI F20 S-TWIN instrument) were applied for the structural characterization of the resulting nanosheets. X-ray diffraction (XRD) patterns were recorded on a PANalytical X'Pert spectrometer using the Co Kα radiation (λ = 1.78897 Å), and the data were changed to Cu Kα data. N_2 adsorption-desorption analysis was measured on a Micro-meritics Tristar II 3020 instrument (USA). The pore size distributions of the as-prepared samples were analyzed using the Barrett Joyner Halenda (BJH) method. Differential pulse voltammetry (DPV) and electrochemical impedance spectroscopy (EIS) performed with a LK2006 Electrochemical Work Station (Tianjin Lanlike Electronic Co., LTD, Tianjin, China). A three-electrode system, composing a platinum wire as auxiliary electrode, a glassy carbon electrode (GCE, φ3mm) as working electrode and Ag/AgCl reference electrode (sat. KCl) was utilized to carry on all electrochemical processes. The pH measurements were carried out on PHS-3C exact digital pH metre (Shanghai Leici Co. Ltd., China), which was calibrated with standard pH buffer solutions.

2.3. Synthesis of ultrathin $NiCo_2O_4$ nanosheets with mesoporous structure

Typically, 2 mmol of $Co(NO_3)_2 \cdot 6H_2O$, 1 mmol of $Ni(NO_3)_2 \cdot 6H_2O$ and 4.5 mmol of hexamethylenetetramine were dissolved in the mixture of 20 mL ethanol and 40 mL deionized (DI) water and then transferred into 100 mL Teflon-lined. After magnetic stirring for 24 h at 90 °C and cooled to room temperature, the precipitates were separated by centrifugation and washed with DI water and ethanol for three times, respectively. Then final product was obtained after dried in the blast oven for 12 h at 60 °C and annealed the product at 350 °C for 2 h in air.

2.4. Formation of $NiCo_2O_4$-PAMAM/GCE

Firstly, 50 mg of synthesized $NiCo_2O_4$ nanosheets was mixed with 3% PAMAM and then dispersed in 10 mL ultrapure water under ultrasonic while stirring for 1 h. Afterwards, the $NiCo_2O_4$ -PAMAM suspension was dialyzed using a cellulose dialysis sack to purify the product. Washing the collected products with ethanol and ultrapure water respectively for several times and 1.0 mg $NiCo_2O_4$ -PAMAM was re-dispersed in 1.0 mL water for further use. Finally, 4 μL of this mixture was spin-coated onto the interface of the electrode and dried under the infrared lamp to obtain $NiCo_2O_4$-PAMAM modified GCE ($NiCo_2O_4$-PAMAM/GCE).

2.5. Synthesis of g-C_3N_4 nanocomposite

The g-C_3N_4 nanocomposite was synthesized as the reference showed with a minor modification [18]. Dicyandiamide was heated with a ramp rate of 2.3 °C/min for 4 h at 550 °C and cooled at a rate of 1 °C/min. The collected yellow resultant was put into a mortar and milled into powder to obtain bulk g-C_3N_4. After 400 mg of bulk g-C_3N_4 was put into an open ceramic container and heated with a ramp rate of 5 °C/min for 2 h at 550 °C, the g-C_3N_4 nanocomposite, light yellow powder, was obtained.

2.6. Preparation of g-C_3N_4 labeled peptide solution

The g-C_3N_4 labeled peptide solution was prepared as following steps: firstly, 10 mg of PTCA was added into 1 mL doubly distilled water, stirred and mixed with 1 mg mL^{-1} g-C_3N_4, followed by an overnight incubation at 4 °C and ultrafiltration, centrifugation and redispersion using ultrapure water for purification. Next, 20 mM EDC/NHS was added in the resultant solution to realize the connection of PTCA and peptide. Later, 1 mg mL^{-1} peptide was dissolved in 10 mL PBS, stirred and added to the above mixture for overnight at 4 °C temperature. The labeled peptide was purified using 50 mM phosphate buffer solution containing 0.15 M NaCl (pH 7.2) with the same method above.

2.7. Fabrication of the peptide-based sensor

Before modification, the bare GCE was polished with 0.3 μm alumina particles on chamois, then washed with ethanol and water repetitiously and natural dried in air. Next, the mixture of synthesized $NiCo_2O_4$ nanosheets and PAMAM containing 1 mL ultrapure water was spin-coated onto the interface of the electrode, and dried at room temperature under the infrared lamp to obtain $NiCo_2O_4$-PAMAM modified GCE ($NiCo_2O_4$-PAMAM/GCE). Then the modified electrode was incubated in the resulting mixture g-C_3N_4-PTCA-peptide solution at 4 °C for 1 h and softly rinsed with ultrapure water. Subsequently, the electrode was incubated with peptide labeled by g-C_3N_4. This obtained modified electrode was noted as GCE/$NiCo_2O_4$/PAMAM-peptide@g-C_3N_4. Subsequently, the resulting peptide-based sensor was incubated with 5 μL 1 wt% BSA for 50 min at 4 °C to block possible remaining active sites and avoid the non-specific adsorption. Finally, the peptide-based sensor was obtained after softly rinsed with ultrapure water and stored in refrigerator for further use.

2.8. Preparation of clinical samples

Serum samples of healthy persons were provided by Fujian Provincial Hospital and measured by some procedures of trypsin activity detection which include centrifugation (6000 rpm, 5 min) of the fresh blood samples. Before a trypsin test, different concentrations of serum samples need to be diluted 10 times.

3. Results and discussion

3.1. Characterization of $NiCo_2O_4$

The typical SEM and TEM were employed to characterize the structure of $NiCo_2O_4$. From Fig. 1A, it can be clearly seen that numerous nanosheets interconnected with each other were formed, which showed porous nature of nanosheets. In addition, the TEM image displayed in Fig. 1B further verified the $NiCo_2O_4$ nanosheets were composed of nanoparticle subunits. In addition, the HRTEM image exhibited lattice fringes with main interplanar spacing of ca. 0.25 nm, corresponding to the (311) crystal plane of

Please cite this article in press as: Y. Lin, et al., A highly sensitive peptide-based biosensor using $NiCo_2O_4$ nanosheets and g-C_3N_4 nanocomposite to construct amplified strategy for trypsin detection, Analytica Chimica Acta (2018), https://doi.org/10.1016/j.aca.2018.06.040

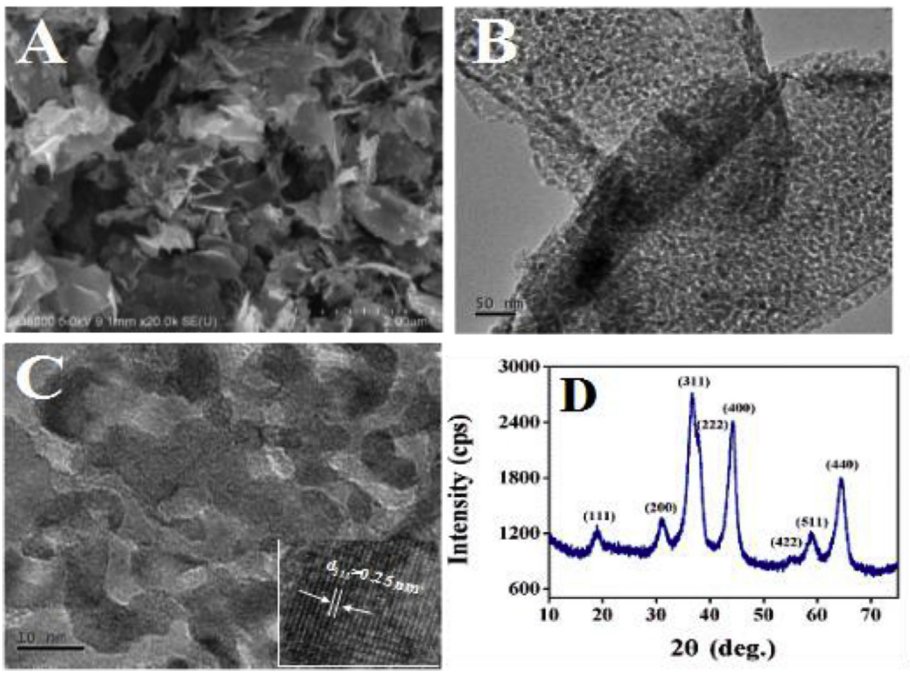

Fig. 1. (A) SEM, (B) TEM and (C) HRTEM imagines and (D) XRD pattern of $NiCo_2O_4$ nanoparticle subunits.

spinel $NiCo_2O_4$ (Fig. 1C). To further obtain the crystalline structure of the $NiCo_2O_4$, the XRD was performed in Fig. 1D, eight distinct diffraction peaks were appeared at 2q values of 19.3, 31.2, 36.8, 38.5, 44.8, 55.8, 59.3 and 65.2, which were in agreement with the (111), (200), (311), (222), (400), (422), (511) and (440) crystal planes of $NiCo_2O_4$ (JCPDS No. 20−0781), respectively [20]. Moreover, no other peaks appeared in the XRD pattern, indicating the $NiCo_2O_4$ nanosheets are pure.

3.2. Electrochemical characterization of peptide-based sensor

In this work, $NiCo_2O_4$-PAMAM as an amplification platform were employed to enhance the electrochemical signal. Therefore, the performance of the peptide-based sensor was investigated by differential pulse voltammetry (DPV) measurement. As shown in Fig. 2A, the DPV response from the $NiCo_2O_4$-PAMAM modified electrode (curve b) was 4 times higher than that of bare glassy carbon electrode ("signal amplify", curve a). The results may be ascribed to the unique structure of $NiCo_2O_4$-PAMAM composite with Ni^{3+} cations in octachedral sites of the Co_3O_4, which permitted the transportation of ions/electrons easier [13,21]. However, when g-C_3N_4 labeled peptides were grafted to the $NiCo_2O_4$-PAMAM modified electrode, an apparent decreased peak current was observed ("signal-off", curve c). This phenomenon can be explained by the wide band gap (about 2.6 eV) of g-C_3N_4 and the contact resistance between the g-C_3N_4 nanosheets, which generated great hindrance and further limited the process of electron transportation [22]. Then an increase of the signal can be clearly seen ("signal-on", curve d) after the modified electrode was incubated with trypsin, indicating the trypsin specifically and effectively cleaved the C-terminal side of arginine in the peptide and made the g-C_3N_4 drop off from the electrode surface. The results showed that the modified electrodes were synthesized successfully.

Furthermore, a contrast experiment was conducted to prove the g-C_3N_4 could significantly decrease the DPV response and the results were showed in the insert of the Fig. 2A. Compared with the DPV signal of the newly constructed peptide−based biosensor (curve c) and the signal of ultrapure water (curve e), there was no evident difference between them, implying the wide band gap and the connect resistance of g-C_3N_4 nanocomposite could hinder the transportation of electrons. This blank experiment also demonstrated that g-C_3N_4 was able to decline the background signal.

Electrochemical impedance spectroscopy (EIS) was used to illustrate the detail fabrication process of the biosensor. The typical impedance spectrum includes a semicircle portion at higher frequency range corresponding to the electron-transfer-limited process and a linear part at lower frequency rang corresponding to the diffusion-limited process [23]. Here, EIS was performed in PBS (0.1 M, pH 7.4) solution containing 5 mM $[Fe(CN)_6]^{3-/4-}$in a frequency range from 0.1 Hz to 100 kHz and the results were displayed in Fig. 2B. The impedance spectrum exhibited an obvious semicircle at high frequency when there was only bare GCE, which indicated that electron could transfer at a low speed (Fig. 2B, curve a). With the $NiCo_2O_4$-PAMAM composite dripped on the surface of bare GCE, the radius of the semicircle evidently decreased, which suggested that the $NiCo_2O_4$-PAMAM on the electrode reduced the surface resistance (Fig. 2B, curve b). This was because the special structure of $NiCo_2O_4$ nanosheets induced the better electronic conductivity and higher electrochemical activity than GCE. After peptides with g-C_3N_4 nanocomposite were anchored onto the PAMAM-$NiCo_2O_4$, the Ret value immediately increased (Fig. 2B, curve c), which demonstrated that g-C_3N_4 blocked the electron transfer tunnel due to its poor electric conductivity. Finally, when the trypsin was incubated on the electrode, a remarkable decrease in the Ret value was observed (Fig. 2B, curve d), implying that the trypsin cleaved the C-terminal side of arginine in the peptide owing to its specific recognition with peptide [10]. The results also indicated the modified electrodes were fabricated successfully.

Moreover, to evaluate the performance of signal restraint resulted from the g-C_3N_4 riveted on peptide, the experiments were conducted to compare the signal responses in the presence and absence of g-C_3N_4 modified on the electrodes in 0.1 mM

Please cite this article in press as: Y. Lin, et al., A highly sensitive peptide-based biosensor using $NiCo_2O_4$ nanosheets and g-C_3N_4 nanocomposite to construct amplified strategy for trypsin detection, Analytica Chimica Acta (2018), https://doi.org/10.1016/j.aca.2018.06.040

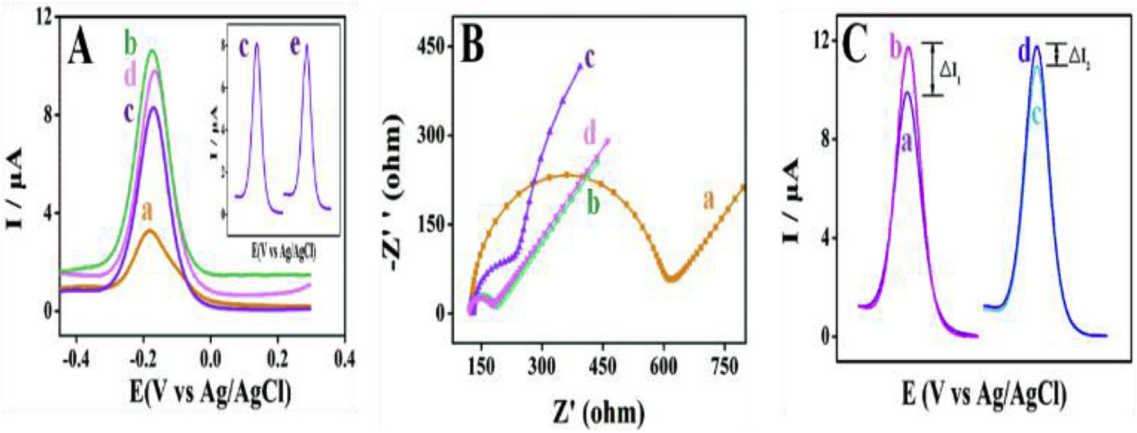

Fig. 2. (A) Differential pulse voltammograms obtained at different electrodes in 0.1 mM $[Ru(NH_3)_6]^{3+}$ containing 1.0 M KCl. (B) Nyquist diagrams of EIS (in the frequency range of 0.1 Hz−10 kHz) obtained at different electrodes in the 5.0 mM $K_3Fe(CN)_6/K_4Fe(CN)_6$ (1:1) containing 1.0 M KCl. (a) GCE (b) GCE/$NiCo_2O_4$/PAMAM (c) GCE/$NiCo_2O_4$/PAMAM-peptide@g-C_3N_4 (d) the electrode of (c) incubated with trypsin. Inset, (e) DPV response of electrode (c) incubated with ultrapure water. (C) Differential pulse voltammograms of the electrode (a) GCE/$NiCo_2O_4$/PAMAM-peptide@g-C_3N_4 before and after incubated with trypsin (b), and the electrode of (c) GCE/$NiCo_2O_4$/PAMAM-peptide before and after incubated with trypsin (d).

$[Ru(NH_3)_6]^{3+}$ containing 1 M KCl. As shown in Fig. 2C, the electrochemical signal of peptide-based sensor with g-C_3N_4 (curve a) was lower than that of without g-C_3N_4 (curve c). After the electrode was incubated with trypsin to cleave the specific site of peptide, both of the signals from peptide-based sensor with g-C_3N_4 (curve b) and without g-C_3N_4 (curve d) were increased. However, the amplitude of the current responses (△I) changed more when g-C_3N_4 existed. The above results confirmed the g-C_3N_4 could improve the sensitivity of sensor by restraining the electron transportation resulted from the poor electric conduction of g-C_3N_4 [18]. This strategy illustrated an indirect signal amplification method which exhibited highly improved sensitivity than without g-C_3N_4 labeling peptide-based sensor.

3.3. Optimization of experimental conditions

In order to maximize the peptide-based sensor response, several experimental conditions including the amount of $NiCo_2O_4$ and PAMAM, incubation time between peptide and trypsin, the effect of pH on the process of trypsin cleaving peptide, and the trypsin incubation temperature were optimized. The amount of PAMAM and $NiCo_2O_4$ played important roles in electron transportation on the surface of electrode, so it was necessary to investigate the effect caused by amount of PAMAM and $NiCo_2O_4$. The DPVs of electrodes modified with different concentrations of PAMAM and $NiCo_2O_4$ were performed in 1.0 M KCl containing 0.1 mM $[Ru(NH_3)_6]^{3+}$. It was clear that the DPV peak current of $[Ru(NH_3)_6]^{3+}$ increased with the elevating concentration of PAMAM from 0.1 to 0.3 wt% and then decreased because the thick PAMAM layers on the electrode hindered the electron transfer (Fig. 3A). As shown in Fig. 3B, the peak current reached a maximum when the amount of $NiCo_2O_4$ was 5 mg mL^{-1}. Under this circumstance, $NiCo_2O_4$ has better electronic conductivity and higher electrochemical activity [15]. Whereas, with the continue increasing of $NiCo_2O_4$ from 5 to 7 mg mL^{-1}, the peak current rapidly decreased due to the thick layers of $NiCo_2O_4$ impeded the electron transfer on the surface of electrode. Therefore, 0.3 wt% PAMAM and 5 mg mL^{-1} $NiCo_2O_4$ were chosen to modify the electrode in the following experiments.

The incubation time was an important parameter for the proposed peptide-based sensor during the trypsin detection. In order to figure out the best incubation time, the electrodes were first incubated with 1 mg mL^{-1} peptide for 15, 30, 45, 60, and 75 min, respectively, and the responses of peptide were recorded as I_0. Then, the electrodes were continued to incubate with 1 μg mL^{-1} trypsin for 1 h, and the responses of trypsin were recorded as I_1. The variable responses of before and after trypsin cleaving peptide were recorded as △I. This signal record method exactly illustrated the trend of responses under different experimental conditions. Fig. 4A showed that the current changes increased with the extension of incubation time from 15 to 60 min and then decreased. Thus 60 min was chosen for subsequent experiments. With the same assay method, the incubation time of trypsin was also investigated for 15, 30, 45, 60, and 75 min, respectively. The results displayed that the amplitude of the response increased with cleavage peptide time from 15 min to 45 min (Fig. 4B), and then declined with further increase of cleavage peptide time. Therefore, 45 min was selected as the optimal incubation time for the determination of trypsin in subsequent experiments.

The pH value of the detection solution was also optimized since unsuitable pH may cause protein denaturalization, which would affect the electrochemical response of the peptide-based sensor. In order to optimize the pH value, a series of Tris-HCl with the pH values ranged from 7.0 to 9.0 and containing 1.0 μg mL^{-1} trypsin solution were prepared and the peptide-based sensors were tested in 1.0 M KCl with 0.1 mM $[Ru(NH_3)_6]^{3+}$ using DPVs. Fig. 4C displayed the variable value increased with increasing pH and reached a maximum at pH 8.5. Therefore, 8.5 were chosen as the optimal pH value in the following experiments. In addition, the temperature of the trypsin cleaving peptide efficiency also greatly affected the analytical performance of the proposed peptide-based assay. As described in Fig. 4D, the signal of trypsin reached a top point when the incubation temperature was up to 37 °C and then decreased with further increase of incubation temperature. This might attribute to the fact that the higher temperature partly caused the denaturation of proteins [24]. Thus, 37 °C was selected as the best incubation temperature for the peptide-based sensor.

3.4. Performance of the peptide-based sensor

As expected, under the optimistic condition, the DPVs peak current of the peptide-based sensor increased with the increasing concentration of trypsin from 10^{-10} to 10^{-4} mg mL^{-1} as shown in Fig. 5A. Fig. 5B showed that the proposed peptide-based sensor has a wide linearity range from 10^{-10} to 10^{-4} mg mL^{-1} with a low

Please cite this article in press as: Y. Lin, et al., A highly sensitive peptide-based biosensor using $NiCo_2O_4$ nanosheets and g-C_3N_4 nanocomposite to construct amplified strategy for trypsin detection, Analytica Chimica Acta (2018), https://doi.org/10.1016/j.aca.2018.06.040

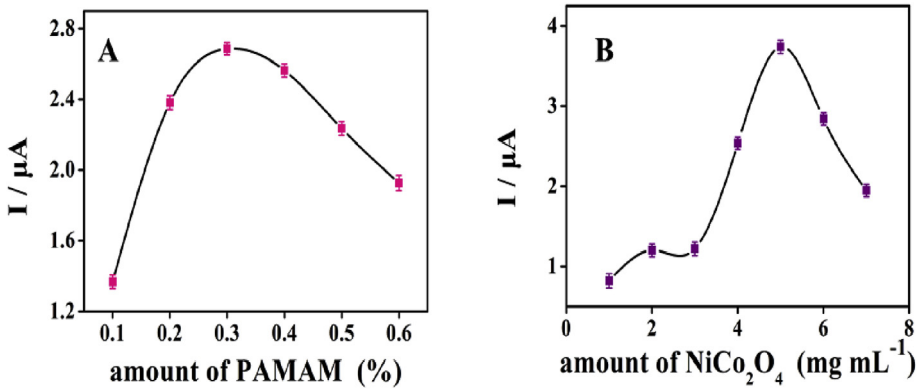

Fig. 3. Current responses to different concentrations of (A) PAMAM and (B)$NiCo_2O_4$ in 0.1 mM $[Ru(NH_3)_6]^{3+}$containing 1.0 M KCl.

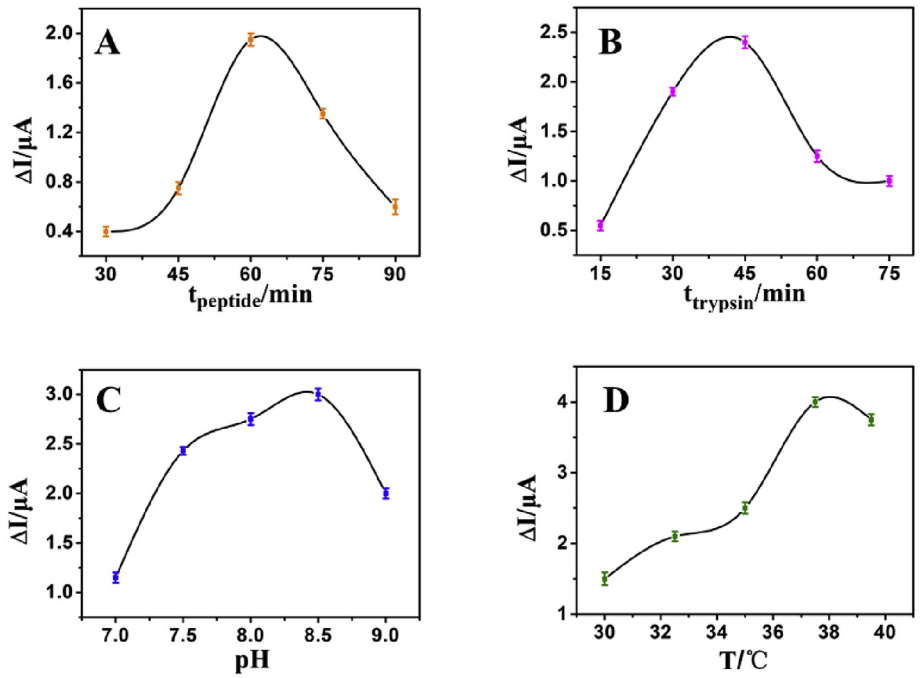

Fig. 4. Effect of (A) the peptide incubation time, (B) the trypsin cleaving time, (C) pH of trypsin cleaving peptide, (D) temperature of trypsin cleaving peptide versus △I (△I = $I_1 - I_0$), I_0 was the signal of GCE/$NiCo_2O_4$/PAMAM-peptide@g-C_3N_4, I_1 was the signal after the modified electrode incubated with trypsin in 0.1 mM $[Ru(NH_3)_6]^{3+}$ containing 1.0 M KCl.

detection limit of 10^{-10} mg mL^{-1}, which indicated the response of different concentration of trypsin cleaving the peptide displayed a good linear calibration plot against the logarithm of trypsin concentration under the optimized conditions. The comparisons of the linear range of different analysis assays were listed in Table 1. Moreover, it could be observed from the inset of Fig. 5B that several electrodes modified in the same way have good reproducibility when the concentration of trypsin was under 10^{-9} mg mL^{-1}.

3.5. Amplification effect of $NiCo_2O_4$ nanosheets

To prove the amplification effect of $NiCo_2O_4$ nanosheets, the comparison of signals from different electrodes modified with $NiCo_2O_4$-PAMAM and PAMAM at different concentration of trypsin was investigated in Fig. 5C. The linear relationships between I_p and the logarithm of trypsin concentration were quantified as the equations.

$$I_{p1}\ (\mu A) = 0.19\ \log c\ (mg\ mL^{-1}) + 7.24,\ (R^2 = 0.9954) \quad (1)$$

with the presence of $NiCo_2O_4$ nanosheets

$$I_{p2}\ (\mu A) = 0.11\ \log c\ (mg\ mL^{-1}) + 4.35,\ (R^2 = 0.9983) \quad (2)$$

with the absence of $NiCo_2O_4$ nanosheets. The results demonstrated the electrode modified with $NiCo_2O_4$-PAMAM showed higher electrochemical signals than that of only PAMAM, indicating $NiCo_2O_4$ nanosheets did amplify the electrochemical signals. Furthermore, the slope of presence $NiCo_2O_4$ nanosheets (curve a) was more acclivitous than that of absence $NiCo_2O_4$ nanosheets (curve b), showing that $NiCo_2O_4$ nanosheets improved the sensitivity of the constructed peptide-based sensor because $NiCo_2O_4$ have excellent electrocatalysis and could effectively transfer electrons [24].

Please cite this article in press as: Y. Lin, et al., A highly sensitive peptide-based biosensor using $NiCo_2O_4$ nanosheets and g-C_3N_4 nanocomposite to construct amplified strategy for trypsin detection, Analytica Chimica Acta (2018), https://doi.org/10.1016/j.aca.2018.06.040

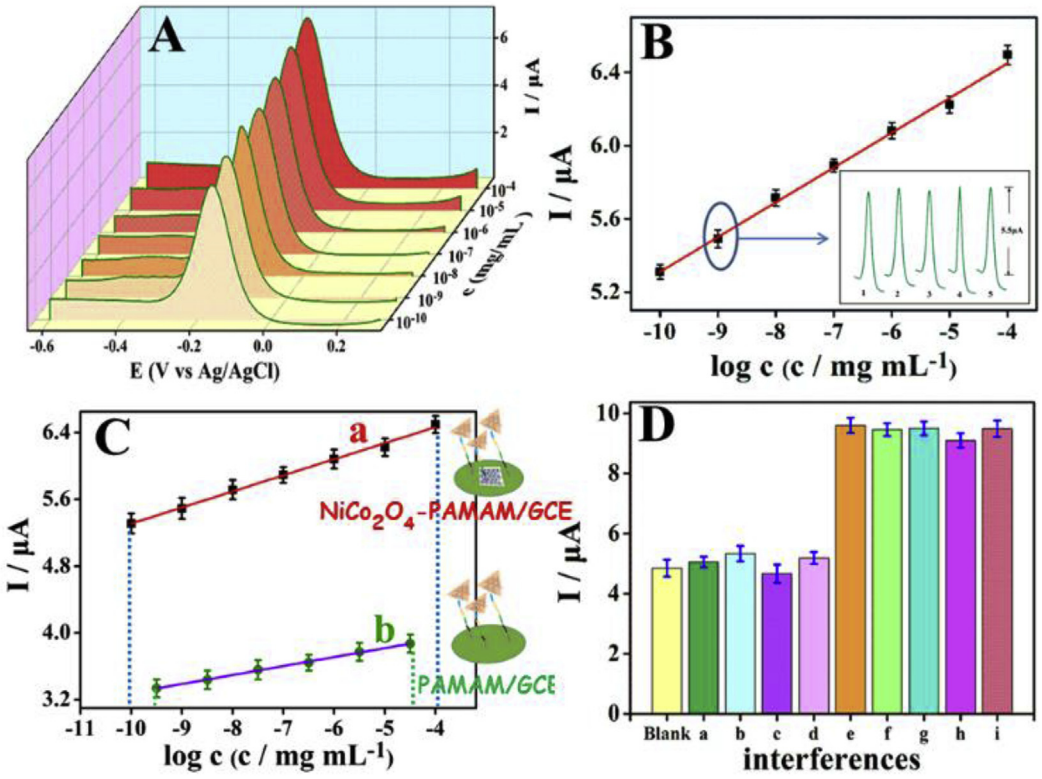

Fig. 5. (A) Differential pulse voltammograms of GCE/$NiCo_2O_4$/PAMAM-peptide@g-C_3N_4 incubated with different concentrations of trypsin from 10^{-4} to 10^{-10} mg mL^{-1}. (B) The calibration curve of the logarithm of trypsin concentration, and the inset was the reproducibility of GCE/$NiCo_2O_4$/PAMAM-peptide@g-C_3N_4 when trypsin concentration was 10^{-9} mg mL^{-1}. (C) The calibration curves of trypsin concentration in presence (curve a) or absence (curve b) $NiCo_2O_4$ on the electrodes. (D) Current response of GCE/$NiCo_2O_4$/PAMAM-peptide@g-C_3N_4 reacted with H_2O (blank), 1.0 mg mL^{-1}HRP (a), BSA (b), AFP (c), Lysozyme (d), 0.01 mg mL^{-1} trypsin (e), 1.0 mg mL^{-1} HRP mixture with 0.01 mg mL^{-1} trypsin (f), BSA mixture with trypsin (g), AFP mixture with trypsin (h), Lysozyme mixture with trypsin (i) in 0.1 mM $[Ru(NH_3)_6]^{3+}$ containing 1.0 M KCl.

Table 1
Results of trypsin determination in normal adult serum samples.

Sample	Trypsin added (ng mL^{-1})	Found (ng mL^{-1})	Recovery (%)	RSD (%, n = 5)
Serum	8.55	8.11	94.9	4.3
	9.0	8.26	91.8	3.7
	13.5	14.02	103.9	2.9

3.6. Selectivity, stability and reproducibility of the peptide-based sensor

To evaluate of selectivity of the electrochemical peptide-based senor, various possible interferences, such as HRP, BSA, AFP and Lysozyme were investigated by examining current responses of GCE/$NiCo_2O_4$/PAMAM-peptide@g-C_3N_4. Briefly, the proposed peptide-based sensor was immersed in the solution of 0.01 mg mL^{-1} trypsin, interference (1.0 mg mL^{-1}), 0.01 mg mL^{-1} trypsin with interference (1.0 mg mL^{-1}), respectively. As presented in Fig. 5D, compared with pure trypsin cleaving peptide, the current responses of each interference were about half of it. On the other hand, only slight signal changes were found after trypsin was mixed with these interferences. These results suggested that the selectivity of the proposed peptide-based sensor was acceptable within experimental error for the determination of trypsin.

To study the reproducibility of peptide-based sensor, the concentration of 1 ng mL^{-1} trypsin solution was measured five times using freshly prepared modified electrode. As depicted in the inset of Fig. 5B, the electrochemical responses were almost consistent, demonstrating the repeatability of the proposed peptide-based sensor was satisfactory. Moreover, the stability of the peptide-based sensor was evaluated by storing the modified electrodes at 4 °C for over 10 days and recording the responses periodically. The results showed that the electrochemical response dropped less than 10% compared with the freshly prepared modified electrode at the end of 10th day, which indicated the proposed peptide-based sensor possessed excellent long-term stability.

3.7. Analysis of clinical serum samples

To test the availability of the proposed peptide-based sensor in clinical use, three serum samples containing trypsin was examined. The results were shown in Table 1. As a matter of fact, a satisfactory recovery in the range from 91.78% to 103.85% was observed, and the RSD (n = 5) was less than 4.3%. Thus, the proposed peptide-based sensor showed the potential application in clinical diagnostics for simultaneous determination of trypsin.

3.8. The effect of trypsin inhibitor

To assess the reproducibility, Trypsin inhibitor was used to further verify the practicability of the strategy because the trypsin would disassemble when corresponding trypsin inhibitors were

Please cite this article in press as: Y. Lin, et al., A highly sensitive peptide-based biosensor using $NiCo_2O_4$ nanosheets and g-C_3N_4 nanocomposite to construct amplified strategy for trypsin detection, Analytica Chimica Acta (2018), https://doi.org/10.1016/j.aca.2018.06.040

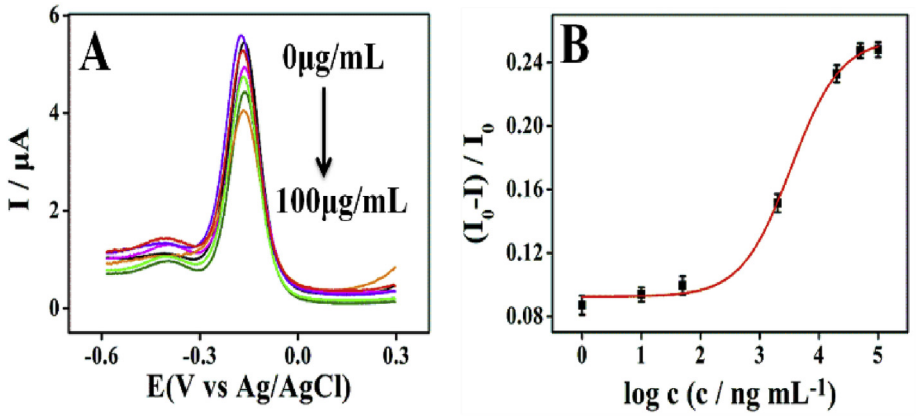

Fig. 6. (A) DPVs of 0.1 mg mL^{-1} trypsin incubated with 0, 0.01, 0.05, 2, 20, 50, 100 μg mL^{-1} inhibitor for 1 h at GCE/$NiCo_2O_4$/PAMAM-peptide@g-C_3N_4. (B) The relationship between the inhibitor efficiency ($(I_0 - I)/I_0$) and the logarithm of inhibitor concentration, I_0 was the signal of 0.1 mg mL^{-1} trypsin, I was the signal of 0.1 mg mL^{-1} trypsin incubated with different concentration inhibitor at GCE/$NiCo_2O_4$/PAMAM-peptide@g-C_3N_4 in 0.1 mM $[Ru(NH_3)_6]^{3+}$ containing 1.0 M KCl.

present. The preparative electrodes of GCE/$NiCo_2O_4$/PAMAM-peptide@g-C_3N_4 were incubated with trypsin in different concentrations of trypsin inhibitor for 45 min at 37 °C and the responses were recorded as shown in Fig. 6A. The signals of DPVs decreased with increasing the inhibitor concentration, suggesting the inhibitor effectively retarded trypsin activity. The relationship between the inhibitor efficiency ($(I_0 - I)/I_0$) and the logarithm of inhibitor concentration was displayed in Fig. 6B, where I_0 was the signal of 0.1 mg mL^{-1} trypsin and I was the signal of 0.1 mg mL^{-1} trypsin incubated with different concentration of inhibitor. The fitting curve is a Boltzmann sigmoid and follow the equation [2]:

$$y = A_2 + (A_1\text{-}A_2)/(1 + \exp(x\text{-}x_0)/dx)\ (A_1 = 0.0927,\ A_2 = 0.2543,\ x_0 = 3.5269,\ dx = 0.4114,\ R^2 = 0.9969) \quad (3)$$

Obviously, when the concentration of inhibitor was 2.0 μg mL^{-1}, the slope of this curve reached a maximum value, showing that 50% inhibitory concentration is 2.0 μg mL^{-1}. This result showed the proposed biosensor was accessible and could be employed to detect the trypsin activity and the inhibitor-screening.

4. Conclusions

In conclusion, a new peptide-based sensing platform was established by using $NiCo_2O_4$ nanosheets as amplified strategy to determine a digestive enzyme, trypsin. The peptide-based sensor with direct transduction of a signal corresponding to peptide cleavage events into an electronic signal and provided a simple and sensitive method for determination of trypsin activity. This fabricated peptide-based sensor performed not only a broad linear range with low detection limit of 10^{-10} mg mL^{-1}, but high stability, excellent selectivity and acceptable reproducibility. Furthermore, the accurate results for trypsin activity detection of serum sample revealed a promising platform for clinical diagnostics. Importantly, this is the first time that nanocomposite combined with peptide-based strategy was employed in designing electrochemical biosensor, which could provide a promising perspective in the construction of versatile electrochemical platforms.

Acknowledgements

This project was financially supported by NSFC (21575024, 21205016), National Science Foundation of Fujian Province (2016J06003, 2016J05026, 2017J01620, 2016J01429, 2017J01278), Education Department of Fujian Province (JK2016009, FBJG20170186,JA14071), Foundation of Fuzhou Science and Technology Bureau (2013-S-113) and Key Clinical Specialty Discipline Construction Program of Fujian.

Appendix A. Supplementary data

Supplementary data related to this article can be found at https://doi.org/10.1016/j.aca.2018.06.040.

References

[1] M. Stoytcheva, R. Zlatev, S. Cosnier, M. Arredondo, B. Valdez, High sensitive trypsin activity evaluation applying a nanostructured QCM-sensor, Biosens. Bioelectron. 41 (2013) 862–866.
[2] P. Miao, T. Liu, X. Li, L. Ning, J. Yin, K. Han, Highly sensitive, label-free colorimetric assay of trypsin using silver nanoparticles, Biosens. Bioelectron. 49 (2013) 20–24.
[3] A. Schuchert-Shi, P.C. Hauser, Peptic and tryptic digestion of peptides and proteins monitored by capillary electrophoresis with contactless conductivity detection, Anal. Biochem. 387 (2009) 202–207.
[4] G.W. Schwert, Y. Takenaka, A spectrophotometric determination of trypsin and chymotrypsin, Biochim. Biophys. Acta 16 (1955) 570–575.
[5] R.M. H, Marvin B. Rhodes, Robert E. Feeney, Spectrophotometric determination of trypsin and trypsin inhibitors, Anal. Chem. 29 (1957) 3.
[6] M. Stoytcheva, R. Zlatev, S. Cosnier, M. Arredondo, Square wave voltammetric determination of trypsin activity, Electrochim. Acta 76 (2012) 43–47.
[7] L. Zhang, J. Du, A sensitive and label-free trypsin colorimetric sensor with cytochrome c as a substrate, Biosens. Bioelectron. 79 (2016) 347–352.
[8] Y. Zhou, Q. Xie, Hyaluronic acid-coated magnetic nanoparticles-based selective collection and detection of leukemia cells with quartz crystal microbalance, Sensor. Actuator. B Chem. 223 (2016) 9–14.
[9] Y.-Z. Wang, N. Hao, Q.-M. Feng, H.-W. Shi, J.-J. Xu, H.-Y. Chen, A ratiometric electrochemiluminescence detection for cancer cells using g-C3N4 nanosheets and Ag–PAMAM–luminol nanocomposites, Biosens. Bioelectron. 77 (2016) 76–82.
[10] Q. Yi, Q. Liu, F. Gao, Q. Chen, G. Wang, Application of an electrochemical immunosensor with a MWCNT/PDAA modified electrode for detection of serum trypsin, Sensors 14 (2014) 10203–10212.
[11] X. Gao, G. Tang, Y. Li, X. Su, A novel optical nanoprobe for trypsin detection and inhibitor screening based on Mn-doped ZnSe quantum dots, Anal. Chim. Acta 743 (2012) 131–136.
[12] C. Wang, H. Qi, X. Qiu, Q. Gao, C. Zhang, Homogeneous electrogenerated chemiluminescence peptide-based method for determination of troponin I, Anal. Meth. 4 (2012) 2469–2474.
[13] J. Yang, M. Cho, Y. Lee, Synthesis of hierarchical NiCo2O4 hollow nanorods via sacrificial-template accelerate hydrolysis for electrochemical glucose oxidation, Biosens. Bioelectron. 75 (2016) 15–22.
[14] M. Yu, J. Chen, J. Liu, S. Li, Y. Ma, J. Zhang, J. An, Mesoporous NiCo2O4 nanoneedles grown on 3D graphene-nickel foam for supercapacitor and methanol electro-oxidation, Electrochim. Acta 151 (2015) 99–108.
[15] Z. Yu, H. Li, X. Zhang, N. Liu, W. Tan, X. Zhang, L. Zhang, Facile synthesis of NiCo2O4@Polyaniline core-shell nanocomposite for sensitive determination of glucose, Biosens. Bioelectron. 75 (2016) 161–165.
[16] B. Kavosi, R. Hallaj, H. Teymourian, A. Salimi, Au nanoparticles/PAMAM

dendrimer functionalized wired ethyleneamine-viologen as highly efficient interface for ultra-sensitive alpha-fetoprotein electrochemical immunosensor, Biosens. Bioelectron. 59 (2014) 389–396.
[17] Y. Zhuo, N. Liao, Y.-Q. Chai, G.-F. Gui, M. Zhao, J. Han, Y. Xiang, R. Yuan, Ultrasensitive apurinic/apyrimidinic endonuclease 1 immunosensing based on self-enhanced electrochemiluminescence of a Ru(II) complex, Anal. Chem. 86 (2014) 1053–1060.
[18] H. Gu, T. Zhou, G. Shi, Synthesis of graphene supported graphene-like C3N4 metal-free layered nanosheets for enhanced electrochemical performance and their biosensing for biomolecules, Talanta 132 (2015) 871–876.
[19] N. Garg, M. Basu, A.K. Ganguli, Nickel cobaltite nanostructures with enhanced supercapacitance activity, J. Phys. Chem. C 118 (2014) 17332–17341.
[20] K. Zhou, Z. Hong, C. Xie, H. Dai, Z. Huang, Mesoporous NiCo2O4 nanosheets with enhance sodium ion storage properties, J. Alloy. Comp. 651 (2015) 24–28.
[21] X.-Y. Yu, X.-Z. Yao, T. Luo, Y. Jia, J.-H. Liu, X.-J. Huang, Facile synthesis of urchin-like NiCo2O4 hollow microspheres with enhanced electrochemical properties in energy and environmentally related applications, ACS Appl. Mater. Interfaces 6 (2014) 3689–3695.
[22] F. Zhao, H. Cheng, Y. Hu, L. Song, Z. Zhang, L. Jiang, L. Qu, Functionalized graphitic carbon nitride for metal-free, flexible and rewritable nonvolatile memory device via direct laser-writing, Sci. Rep. 4 (2014) 5882.
[23] F. Zhao, Q. Xie, M. Xu, S. Wang, J. Zhou, F. Liu, RNA aptamer based electrochemical biosensor for sensitive and selective detection of cAMP, Biosens. Bioelectron. 66 (2015) 238–243.
[24] Y. Gu, Q. Wen, Y. Kuang, L. Tang, J. Jiang, Peptide-templated gold nanoclusters as a novel label-free biosensor for the detection of protease activity, RSC Adv. 4 (2014) 13753–13756.

Please cite this article in press as: Y. Lin, et al., A highly sensitive peptide-based biosensor using $NiCo_2O_4$ nanosheets and g-C_3N_4 nanocomposite to construct amplified strategy for trypsin detection, Analytica Chimica Acta (2018), https://doi.org/10.1016/j.aca.2018.06.040